

Dielectric and piezoelectric properties of $(\text{Ba}_{0.95}\text{Ca}_{0.05})(\text{Ti}_{0.88}\text{Zr}_{0.12})\text{O}_3$ ceramics sintered in a protective atmosphere

Su-Wei Zhang, Hailong Zhang*, Bo-Ping Zhang, Gaolei Zhao

School of Materials Science and Engineering, University of Science and Technology Beijing, Beijing 100083, China

Received 22 April 2009; received in revised form 12 June 2009; accepted 24 June 2009

Available online 19 July 2009

Abstract

$(\text{Ba}_{0.95}\text{Ca}_{0.05})(\text{Ti}_{0.88}\text{Zr}_{0.12})\text{O}_3$ (BCTZ) ceramics have been produced in a protective atmosphere of industrial N_2 gas for potential piezoelectric applications. For comparison, the ceramics were also sintered at 1200–1400 °C in air. The results revealed that the reducing atmosphere of $p\text{O}_2 = 5 \times 10^2$ Pa had no substantial effect on the phase structure or the microstructure of the BCTZ ceramics. The XRD patterns suggested a tetragonal to pseudocubic phase transition at sintering temperatures above 1300 °C in both atmospheres. The nitrogen-sintered BCTZ samples had higher dielectric constants ϵ_r but lower electromechanical coupling coefficients k_p than the air-sintered samples. The piezoelectric constant d_{33} for the BCTZ ceramics was not significantly influenced by the reducing atmosphere of $p\text{O}_2 = 5 \times 10^2$ Pa. The correlation of dielectric and piezoelectric properties of the BCTZ ceramics with the sintering temperature was explained based on a competing mechanism between phase structure and microstructure.

© 2009 Elsevier Ltd. All rights reserved.

Keywords: A. Powders-solid-state reaction; C. Dielectric properties; C. Piezoelectric properties; D. BaTiO_3 and titanates; Protective atmosphere

1. Introduction

Co-firing of perovskite materials with base metal electrodes (BMEs) is of interest as it can reduce the production costs of many devices. The two devices which benefit in particular are multilayer ceramic capacitors (MLCCs)¹ and multilayer ceramic actuators.² These devices, however, must be sintered in a reducing atmosphere to prevent oxidation of the electrodes. The (Ca,Zr) co-doped $(\text{Ba}_{0.95}\text{Ca}_{0.05})(\text{Ti}_{0.88}\text{Zr}_{0.12})\text{O}_3$ (BCTZ) ceramics are usually used to produce the high-permittivity dielectrics of Y5V serials.³ The BCTZ ceramics have been co-fired with Ni electrodes in reducing atmospheres to produce BME MLCCs for some time.^{4,5}

Piezoelectric materials that can be co-fired with BMEs to produce multilayer ceramic actuators are expected to reduce production costs. Although the perovskite $\text{Pb}(\text{Zr,Ti})\text{O}_3$ (PZT) has been reported to co-fire with base metal Cu under a controlled sintering atmosphere within a special

oxygen partial pressure window,^{6,7} Pb-containing PZT is a pollutant, and the process is technically complicated. Lead-free piezoceramics have been the focus of much interest since Saito et al.⁸ made a breakthrough in the textured $(\text{Na,K})\text{NbO}_3$ ceramics with Li, Ta, and Sb as co-dopants. So far, the development of lead-free piezoceramics has concentrated on $(\text{Na,K})\text{NbO}_3$, $(\text{Bi,Na})\text{TiO}_3$ and BaTiO_3 systems. Jiang et al.⁹ prepared the $\text{Na}_{0.5}\text{K}_{0.5}\text{NbO}_3\text{--LiSbO}_3\text{--BiFeO}_3$ lead-free ceramic which exhibited good electrical properties and high densities using a conventional sintering technique. Zuo et al.¹⁰ obtained a piezoelectric constant d_{33} as high as 400 pC/N by maintaining a fixed amount of Sb dopant in $(\text{Na,K})\text{NbO}_3$. Zhang et al.¹¹ reported a Bi-compensated $(\text{Bi}_{0.5}\text{Na}_{0.5})\text{TiO}_3\text{--}(\text{Bi}_{0.5}\text{K}_{0.5})\text{TiO}_3$ (BNT–BKT) system which showed high piezoelectric and dielectric properties. Besides being a high-permittivity dielectric material, BaTiO_3 is also known as a lead-free piezoelectric material.^{12,13} The maximum piezoelectric constant d_{33} reported for BaTiO_3 ceramics fabricated by conventional sintering is 190 pC/N.¹² Takahashi et al.^{12,13} reported a piezoelectric constant d_{33} as high as 350 pC/N for BaTiO_3 ceramics obtained by microwave sintering. Furthermore, Shao et al.¹⁴ reported a d_{33} of 419 pC/N which

* Corresponding author. Tel.: +86 10 62333140; fax: +86 10 62332336.
E-mail address: hlzhang@mater.ustb.edu.cn (H. Zhang).

was obtained from a conventional solid-state reaction pathway.

Nevertheless, these undoped BaTiO₃ cannot be directly co-fired with base metals. BaTiO₃ becomes a semiconductor when sintered in a reducing atmosphere.¹⁵ This can be effectively suppressed with the addition of dopants. The doping ions enter the A-sites (Ba-sites) or B-sites (Ti-sites) of the perovskite lattice and form acceptor- or donor-type point defects, which strongly trap any oxygen vacancies and conduction electrons. Zhang et al.¹⁶ realized the Ca-doping of B-sites of BaTiO₃ by controlling the atomic ratio of A- to B-sites. Hansen et al.¹⁷ investigated the dielectric properties of acceptor-doped (Ba,Ca)(Ti,Zr)O₃ ceramics sintered in a reducing atmosphere. Albertsen et al.¹⁸ further studied a complex acceptor–donor doping system in (Ca,Mn) co-doped BaTiO₃ ceramics and showed that this can effectively trap oxygen vacancies and conduction electrons at the same time. There are also some reports on the isovalent doping of BaTiO₃ ceramics that are sintered in reducing atmospheres. Cheng and Shen¹⁹ used Ca ions to substitute Ba ions at the A-site of BaTiO₃. Nanakorn et al.²⁰ studied the dielectric and ferroelectric properties of B-site Zr-doped BaTiO₃ ceramics. It is believed that the difference in ionic radius between dopant and cation compresses the crystal structure and prevents the formation of oxygen vacancies during the sintering in a reducing atmosphere.²¹

The above-mentioned doped BaTiO₃ ceramics which can be sintered in reducing atmospheres with base metals exhibit excellent dielectric properties. However, little attention has been paid to the piezoelectric properties of BCTZ ceramics. These ceramics have only been used in dielectric capacitors so far. The present paper deals with (Ba_{0.95}Ca_{0.05})(Ti_{0.88}Zr_{0.12})O₃ ceramics that were produced in a protective N₂ atmosphere and in air. The objective is to address the effect of the atmosphere during sintering and the sintering temperature on phase structure, microstructure, dielectric and piezoelectric properties of the (Ca,Zr) co-doped BaTiO₃ ceramics.

2. Experimental procedure

Conventional solid-state reaction techniques were used to prepare the BCTZ ceramics in this study. Analytical-grade BaCO₃ (99.9%, Xilong Chemical Reagent, China), CaCO₃ (99.9%, Xilong Chemical Reagent, China), TiO₂ (99.9%, Xilong Chemical Reagent, China), and ZrO₂ (99.9%, Xilong Chemical Reagent, China) powders were used as raw materials. The powders were mixed to give the nominal composition of (Ba_{0.95}Ca_{0.05})(Ti_{0.88}Zr_{0.12})O₃³ and ground by ball milling for 4 h with the addition of alcohol. After drying, the mixture powders were calcined at 1200 °C for 6 h in air. The synthesized BCTZ powders were mixed with a polyvinyl alcohol (PVA) binder solution and then die-pressed at 200 MPa, resulting in disk samples with dimensions of Ø 10 mm × 1 mm. After burning out the binder at 700 °C for 30 min, the samples were sintered at a temperature from 1200 to 1400 °C for 2 h in air or in industrial N₂ gas (oxygen content: 0.5%). For the case of nitrogen gas sintering the chamber pressure was maintained at close to atmospheric pressure, giving an oxygen partial pressure of $p_{\text{O}_2} = 5 \times 10^2$ Pa.

The crystalline structure of the sintered samples was analyzed using X-ray diffraction (XRD) with Cu K α radiation ($\lambda = 1.5416 \text{ \AA}$) filtered through Ni foil (Rigaku, RAD-B system, Tokyo, Japan). The microstructure was observed using a scanning electron microscope (SEM, JSM-6460, Japan). The grain size was obtained by the linear intercept method. The bulk density was measured by the Archimedes method. Silver electrodes were fired at 520 °C for 30 min onto both surfaces of the sintered disk samples for electrical measurements. The samples were poled under dc fields of 2–3 kV/mm at room temperature for 30 min in a silicone oil bath. The dielectric properties were measured from –20 to 180 °C, using an Agilent precision impedance analyzer (4294A, Hewlett-Packard, USA). The room temperature dielectric constant was measured using an automatic component analyzer (TH2828S, Tonghui Electronics, China). The piezoelectric constant was measured 24 h after poling using a quasistatic piezoelectric d_{33} testing meter (ZJ-3A, Institute of Acoustics, Beijing, China).

3. Results and discussion

3.1. Phase structure and microstructure

Fig. 1 shows the XRD patterns of the BCTZ ceramics sintered in industrial N₂ gas at different temperatures. The XRD patterns of air-sintered BCTZ samples were similar to those sintered in N₂ and are not shown here. This result reflects a negligible effect of the reducing atmosphere of $p_{\text{O}_2} = 5 \times 10^2$ Pa on the solid solubility limit of dopants in this study. As shown in Fig. 1, the samples showed patterns typical of BaTiO₃ (PDF cards #79-2265 and #31-0174 for tetragonal and pseudocubic phase, respectively). It has been reported that X7R-formulated BaTiO₃ ceramics can be produced without structural deterioration under oxygen partial pressures as low as 10^{-6} to 10^{-1} Pa.²² Since the p_{O_2} of 5×10^2 Pa used in this study was much higher than the above values, the N₂ atmosphere has been shown to have no effect on the phase structure of BCTZ ceramics. However, a small amount of a second phase, which was identified as Ba₃Ca₂Ti₂O₉ (PDF card #42-0535), was observed for the sample sintered at 1200 °C. The appearance of Ba₃Ca₂Ti₂O₉ is due to the solid solubility of Ca²⁺ in the Ba-site of BaTiO₃ being small at the relatively low temperature of 1200 °C.²³ The Ba₃Ca₂Ti₂O₉ gradually disappeared from the samples above 1200 °C, due to the increased solid solubility of the Ca²⁺ in the Ba-site with increasing sintering temperature. The maximum solubility of [Ca²⁺_(Ba)] in BaTiO₃ is reportedly as high as 20% at 1300 °C,³ whereas the Ca²⁺ concentration was only 5% in this study. As a result, the BCTZ ceramics sintered above 1300 °C possessed a purely perovskite structure. Since Zr⁴⁺ in the Ti-site is an absolute solid solution,²⁰ no second phase containing Zr was observed. These results suggest that Ca²⁺ and Zr⁴⁺ have been successfully incorporated into BaTiO₃ lattices to form a homogeneous solid solution.

The enlargement of the XRD spectra from 2θ of 30° to 33° in Fig. 1 shows that the tetragonal phase is characterized by a (1 0 1)/(1 1 0) peak splitting at about 31.5° for the two samples sintered at 1200 and 1300 °C. When the BCTZ ceramics were

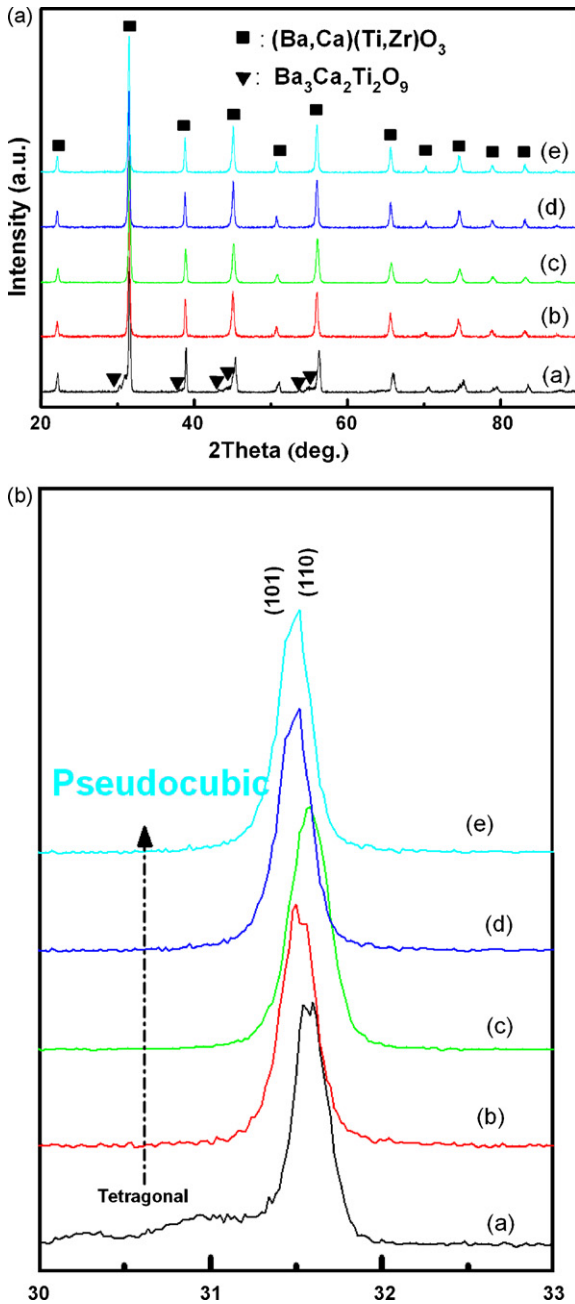


Fig. 1. X-ray diffraction patterns of the BCTZ ceramics sintered in industrial N_2 gas at different temperatures: (a) 1200 °C, (b) 1300 °C, (c) 1320 °C, (d) 1350 °C, and (e) 1400 °C.

sintered above 1320 °C, the phase structure transformed from tetragonal to pseudocubic. The pseudocubic phase is made up of both the orthogonal and tetragonal phases,²⁴ and is caused by the distortion of crystal lattice induced by Ca^{2+} ($r = 0.99 \text{ \AA}$) occupying Ba^{2+} sites (1.34 \AA) and Zr^{4+} ($r = 0.79 \text{ \AA}$) occupying Ti^{4+} (0.68 \AA) sites. With increasing sintering temperature, the pseudocubic peak near 31.5° tends toward lower diffraction angles. This suggests that the occupancy of the dopants in $(Ba,Ca)(Ti,Zr)O_3$ was dependent on sintering temperature. The observed phase transformation for the samples sintered from 1300 to 1320 °C is similar to widely reported polymorphic phase transition (PPT) or morphotropic phase boundary

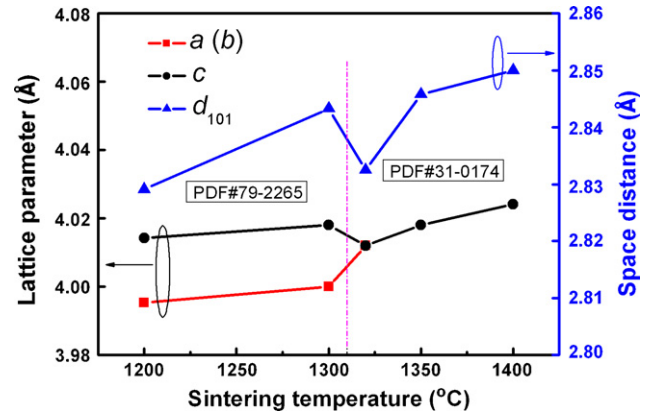


Fig. 2. Dependence of the lattice parameters and space distance of the BCTZ ceramics sintered in industrial N_2 gas on sintering temperature.

(MPB) behavior.^{25–27} This point is supported by the change in the lattice parameters and space distance of BCTZ with sintering temperature.

Fig. 2 shows the dependences of the lattice parameters and space distance of the BCTZ sintered in N_2 with sintering temperature, based on the corresponding data for the diffraction peaks near $2\theta = 31.5^\circ$. The lattice parameters and space distance of the BCTZ samples sintered in air were similar to those sintered in N_2 and are not shown here. As shown in Fig. 2, the lattice parameter c first increased with increasing sintering temperature from 1200 to 1300 °C, then decreased abruptly at 1320 °C, before continuing to increase from 1320 to 1400 °C. The variation of space distance d_{101} was similar to that of lattice parameter c . The changes in the lattice parameters and space distance are consistent with shifts in the observed diffraction peaks at the sintering temperature of 1320 °C. It suggests that the tetragonal and pseudocubic phases coexist in the BCTZ samples sintered at around 1320 °C. This kind of dual-phase coexistence is due to the distortion of crystal lattice²⁴ that is dependent on sintering temperature. As the ionic radius of Zr^{4+} (0.79 \AA) is larger than that of Ti^{4+} (0.68 \AA), the substitution of Zr^{4+} for Ti^{4+} , at concentrations as high as 12% for Zr^{4+} in this study, could lead to expansion of the $BaTiO_3$ crystals and hence change the lattice parameters. Raising the sintering temperature could promote such substitution and increase the distortion of the BCTZ crystals. Accordingly, the phase transformation of BCTZ resulting from sintering temperature in this study is entirely different from PPT- or MPB-like behavior that is usually due to compositional modification.

Fig. 3 shows the sample density of the BCTZ ceramics sintered in industrial N_2 gas and in air at different temperatures. The theoretical density of BCTZ was calculated to be 5.8899 g/cm^3 according to PDF card #31-0174. The sample densities showed negligible differences between nitrogen- and air-sintered BCTZ ceramics. It suggests that the reducing atmosphere of $pO_2 = 5 \times 10^2 \text{ Pa}$ does not affect the increase in density of the BCTZ ceramics. As shown in Fig. 3, the measured density increased with increasing sintering temperature. The relative density of the ceramics was just 83.5% of the theoretical density when sintered at 1200 °C, whereas it reached 96.0% at 1400 °C.

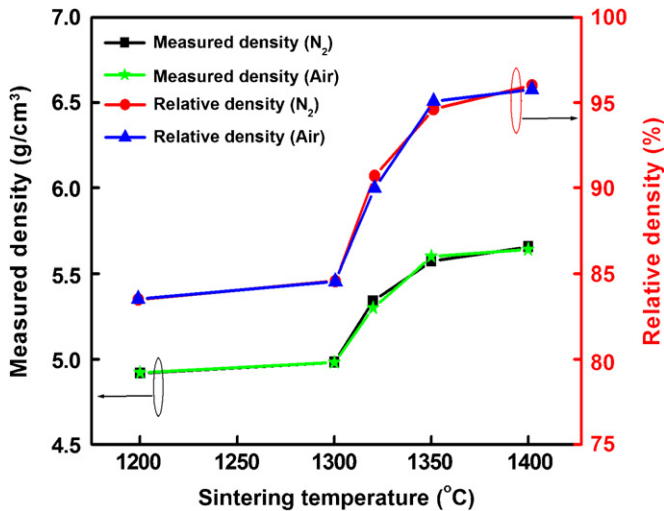


Fig. 3. Measured density and relative density of the BCTZ ceramics sintered in industrial N₂ gas and in air at different temperatures.

That the BCTZ ceramics became more dense should be connected to additional Ca²⁺ entering Ba-site and Zr⁴⁺ entering Ti-site.²⁸ Raising the sintering temperature promotes the diffusion of Ca²⁺ and Ti⁴⁺ and causes the BCTZ ceramics to become more dense.

Fig. 4 shows SEM micrographs of the BCTZ ceramics sintered in industrial N₂ gas and in air at different temperatures. The microstructure of the samples sintered in both atmospheres became more dense and the grain size tended to increase with increasing sintering temperature. The grain size of the nitrogen-sintered BCTZ ceramics at 1200 °C was about ~3.5 μm, and increased to ~5 μm at 1350 °C. At 1400 °C the grains were ~7 μm in size. This is in agreement with the trends in the density shown in Fig. 3. The SEM observations further suggest that increasing the sintering temperature is an effective way to form a dense microstructure with large grains. The microstructure of BCTZ ceramics sintered in both atmospheres showed no substantial variations. The microstructure observations are in agreement with the results of Mn-doped SrTiO₃ ceramics which are also sintered in N₂ and in air.²⁹

3.2. Dielectric and piezoelectric properties

Fig. 5 shows the frequency dependence of the dielectric constant for the BCTZ ceramics sintered in industrial N₂ gas and in air on the sintering temperature. The dielectric constants of the BCTZ ceramics were lower than those of the undoped BaTiO₃ ceramics.³⁰ Victor et al.³¹ also reported that Ca-doped BaTiO₃ ceramics showed lower dielectric constants than BaTiO₃ ceramics. By comparison, the BCTZ ceramics sintered in N₂ had higher dielectric constants than the samples sintered in air. The effect of the sintering atmosphere on dielectric constant will be discussed later.

As shown in Fig. 5, the dielectric constant ϵ_r for all the samples decreased with increasing measuring frequency from 0.1 kHz to 1 MHz. This is associated with some relaxation polarization mechanisms at high frequencies. The decrease in ϵ_r takes

place when the jumping frequency of the electric charge carriers in the sample cannot follow the alternation of the applied electric fields beyond a certain critical frequency.³² The results indicate that at low frequencies and temperatures, ϵ_r has a major contribution from dipoles.³³

The ϵ_r values of the BCTZ ceramics sintered in both atmospheres first increased with increasing sintering temperature and attained a peak value at 1350 °C, and then decreased at 1400 °C to be as low as at 1200 °C. The maximum dielectric constant is usually observed near PPT or MPB in perovskite structured dielectrics.^{25–27} As shown in Figs. 1 and 2, the coexistence of two phases, similar to PPT or MPB behavior, was observed in the BCTZ sample sintered at 1320 °C. Therefore, there should be other mechanisms responsible for the above inconsistency. It has been reported that dielectric constant will decrease with increasing porosity in a dielectric ceramic.^{34,35} Although the BCTZ ceramics sintered at 1320 °C exhibited a PPT-like structure, it also had a relatively porous microstructure, as shown in Fig. 4c. On the other hand, although the BCTZ ceramics sintered at 1400 °C had a dense microstructure, the crystalline structure was far from the PPT-like structure. There should be a competing mechanism between the crystalline structure and the microstructure that is responsible for the correlation of dielectric constant with sintering temperature in this study.

Fig. 6 shows the piezoelectric constant d_{33} and the planar electromechanical coupling coefficient k_p as functions of the sintering temperature for the ceramics. The d_{33} values of the BCTZ ceramics sintered in both atmospheres were almost the same; however, the samples sintered in air showed higher k_p values than the samples sintered in N₂. The BCTZ ceramics sintered in N₂ attained a d_{33} of 200 pC/N and a k_p of 17%.

As shown in Fig. 6, the d_{33} and k_p values of the samples sintered in N₂ and in air all peaked at 1350 °C. It is generally accepted that the maximum piezoelectric constant is attained at a PPT- or MPB-site, especially in the Pb(Zr,Ti)O₃ and (K,Na)NbO₃ systems.^{25–27} On the other hand, it is also reported that the piezoelectric constant is proportional to the grain size^{34,36} and inversely proportional to the porosity of the ceramics.^{35,37} As with the dielectric constant, the maximum d_{33} and k_p values of the BCTZ ceramics are related to the competing mechanisms of the crystalline structure and the microstructure. If the BCTZ ceramics sintered at 1320 °C could be made as dense as those at 1350 °C, they would have the highest piezoelectric properties. The piezoelectric properties of the BCTZ ceramics could be enhanced with a compromise and by further optimizing the doping content of Ca²⁺ and Zr⁴⁺ in the BCTZ ceramics. This will be the subject of a future study. Fig. 7 shows the temperature dependence of the dielectric constant measured at 1 kHz for BCTZ ceramics sintered at 1350 °C in industrial N₂ gas and in air. The BCTZ ceramics exhibited abrupt changes in relative permittivity, which is normal for ferroelectric behavior.²⁴ The transition temperature T_1 from orthorhombic to pseudocubic structure occurred at ~20 °C, and the T_c from pseudocubic to cubic structure occurred at ~85 °C for both samples. McCauley et al.¹⁵ has suggested that the temperature T_m corresponding to the maximum dielectric constant ϵ_r shifts to higher temperatures when BaTiO₃-based dielectrics are sintered in an atmosphere

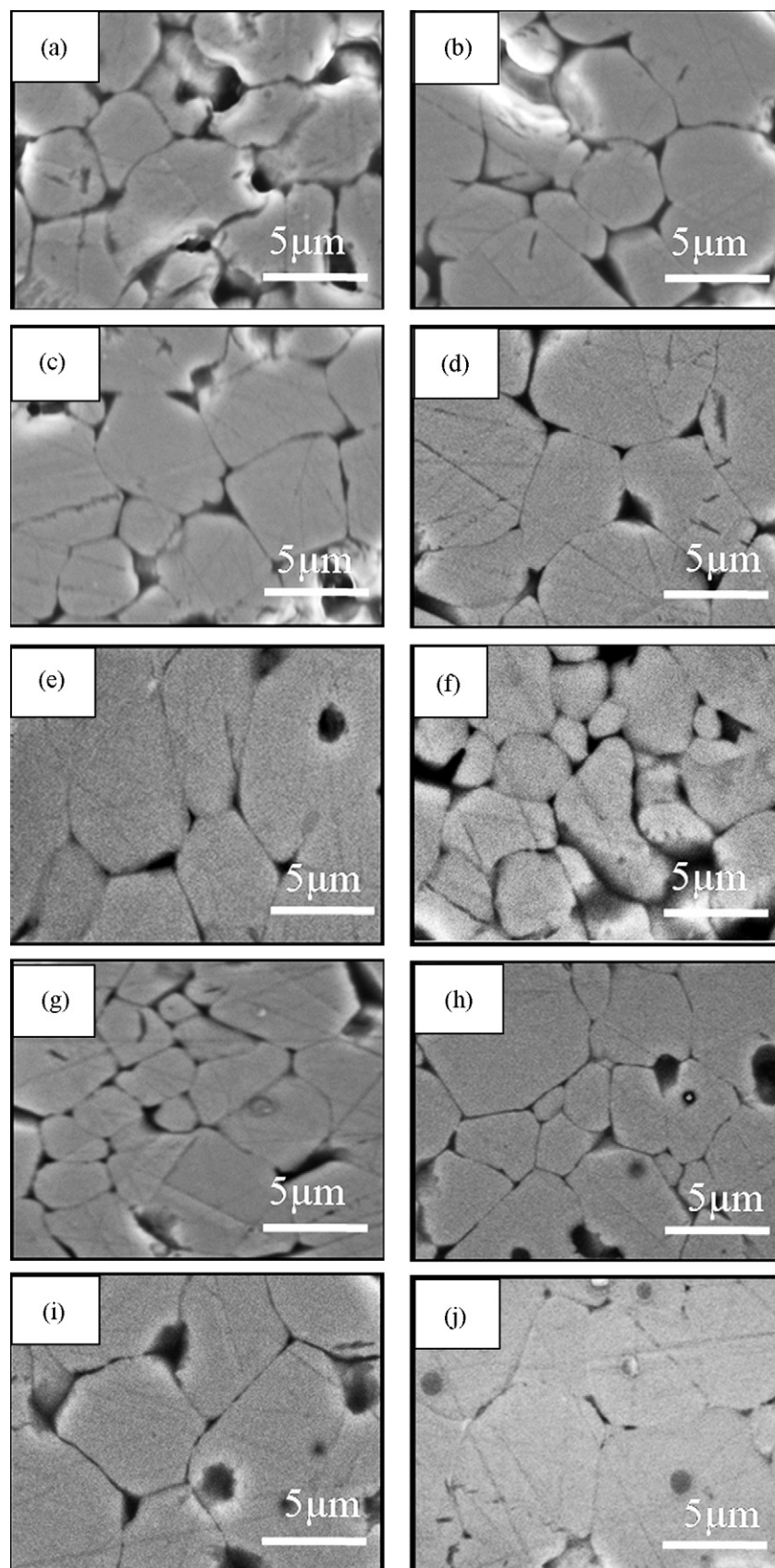


Fig. 4. SEM micrographs of the BCTZ ceramics sintered in industrial N₂ gas (a–e) and in air (f–j) at different temperatures: (a and f) 1200 °C, (b and g) 1300 °C, (c and h) 1320 °C, (d and i) 1350 °C, and (e and j) 1400 °C.

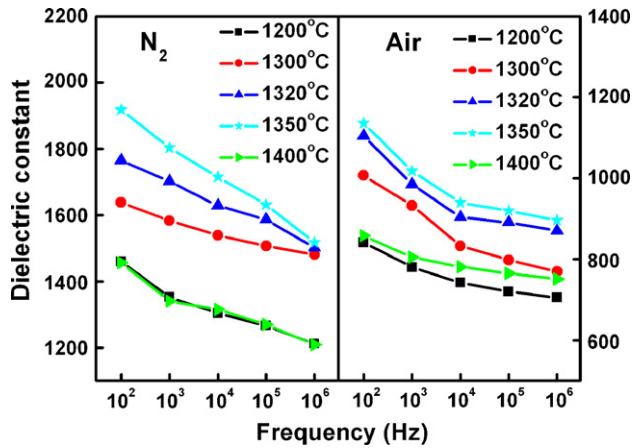


Fig. 5. Frequency dependence of the dielectric constant, ϵ_r , for the BCTZ ceramics sintered in industrial N_2 gas and in air at different temperatures.

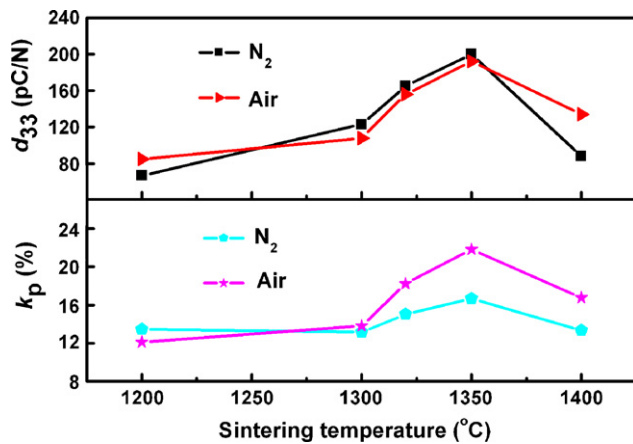


Fig. 6. Piezoelectric constant, d_{33} , and planar electromechanical coupling coefficient, k_p , as functions of the sintering temperature of the BCTZ ceramics sintered in industrial N_2 gas and in air.

with low oxygen partial pressure, and attributed these changes in T_m to the number of oxygen vacancies produced. The sintering atmosphere did not cause appreciable changes in the transition temperature of the BCTZ ceramics in this study. This implies that the number of oxygen vacancies is small

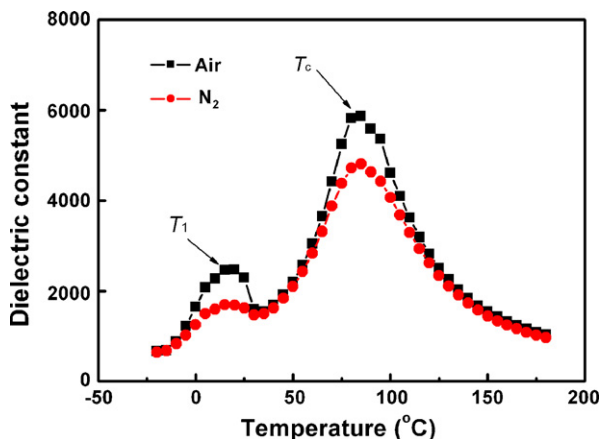


Fig. 7. Temperature dependence of the dielectric constant measured at 1 kHz for the BCTZ ceramics sintered at 1350 °C in industrial N_2 gas and in air.

when BCTZ ceramics were sintered in the N_2 atmosphere of $pO_2 = 5 \times 10^2$ Pa.

Compared with undoped $BaTiO_3$ ceramics sintered in air,³⁰ the T_1 of the BCTZ ceramics sintered in air showed no change, while the T_c shifted from 125 °C to the lower temperature of 85 °C. The shift in the phase transition temperature observed is consistent with the results reported for Ca-doped $BaTiO_3$ ceramics,³¹ and should be closely related to Ca^{2+} occupying the Ba^{2+} site in the BCTZ ceramics.¹⁹ Although the incorporation of Ca^{2+} and Zr^{4+} into Ba- and Ti-sites, respectively, of $BaTiO_3$ has decreased the T_c value, the BCTZ ceramics could still be used over an acceptable temperature range.

3.3. Effects of sintering atmosphere on BCTZ ceramics

Fig. 8 shows an Ellingham diagram of the metal oxides of interest to this study. The data were collected from literature.³⁸ The oxygen partial pressures for the two atmospheres of air and industrial N_2 gas are indicated in the diagram. During sintering, the oxygen partial pressure of the atmosphere was not adjusted and stayed constant at the various sintering temperatures. As shown in Fig. 8, the oxygen partial pressures for both air and N_2 were higher than the pO_2 which corresponds to the deoxidation of TiO_2 , and much higher than that of BaO . Therefore, the $(Ba_{0.95}Ca_{0.05})(Ti_{0.88}Zr_{0.12})O_3$ ceramics sintered in N_2 maintained their perovskite structure. It should be noted that the pO_2 of 5×10^2 Pa for the N_2 atmosphere is also high enough to cause the oxidation of the base metals such as Ni. Although the sintering atmosphere of N_2 did not affect the phase structure of the BCTZ, the oxygen partial pressure would not be compatible with co-firing with Ni. In order to co-fire BCTZ ceramics with base metal electrodes, the oxygen partial pressure of the sintering atmosphere should be reduced to prevent the oxidation of the base metals.

Generally speaking, sintering atmospheres with a low oxygen partial pressure will introduce ionized oxygen vacancies and conduction electrons into perovskite dielectrics according to the following defect chemical reaction:

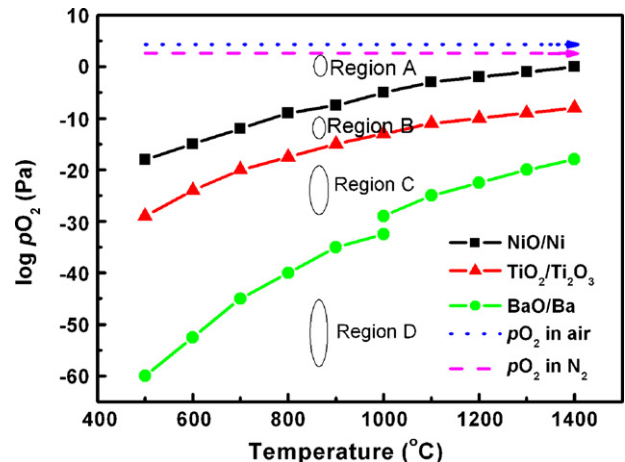
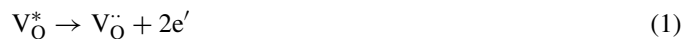
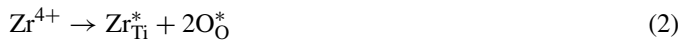


Fig. 8. Phase stability plot of the metal oxides of interest, as a function of temperature and oxygen partial pressure.³⁸

The conduction electrons so produced will give rise to high electronic conductivity in the dielectric material, leading to lower insulation resistance. In this study, the oxygen vacancies and conduction electrons could hence be introduced into the BCTZ ceramics when sintered under the protective atmosphere of N₂. However, during the poling processing it was found that there was no appreciable leakage current observed in the BCTZ samples sintered in both atmospheres with the dc electric fields which were applied. This can be explained as follows. The defect chemical reaction of Zr⁴⁺ substitution for Ti⁴⁺ can be described as



Since the ionic radius of Zr⁴⁺ is larger than that of Ti⁴⁺, the isovalent substitution of Zr for Ti will compact the Ti–O unit cells and prevent oxygen atoms from escaping the perovskite crystals.²¹ The Zr⁴⁺ doping in this study of 12% is capable of making the BaTiO₃ non-reducible in the atmosphere used here. The conductivity caused by electron hopping between Ti⁴⁺ and Ti³⁺ in BaTiO₃ can also be suppressed with the substitution of Ti by Zr.²¹

The dielectric properties of the BCTZ ceramics were affected by the sintering atmosphere used in this study. As shown in Fig. 5, the dielectric constants of samples sintered in N₂ were higher than those sintered in air. This is similar to Mn-doped SrTiO₃.²⁹ The increase in the dielectric constant of the samples sintered in N₂ could be connected to electron relaxation polarization. Although Zr substitution has greatly depressed the production of conduction electrons in (Ba,Ca)(Ti,Zr)O₃ under low oxygen partial pressures, a small amount of weakly bonded electrons could still be produced when the samples were sintered in N₂. The weakly bonded electrons can move a short distance and tend to be oriented with the electric fields applied, and thus contribute to an increase in the dielectric constant.

4. Conclusions

The (Ba_{0.95}Ca_{0.05})(Ti_{0.88}Zr_{0.12})O₃ (BCTZ) ceramics, with a single perovskite phase, were successfully produced by protective sintering in industrial N₂ gas above 1300 °C. The reducing atmosphere of $p_{\text{O}_2} = 5 \times 10^2$ Pa had a negligible effect on the phase structure and microstructure of the BCTZ ceramics. PPT-like behavior was observed for the BCTZ ceramics sintered at around 1320 °C in both N₂ and air atmospheres. The grain size and microstructure of the BCTZ ceramics were increased with increasing sintering temperature from 1200 to 1400 °C. The samples sintered in N₂ exhibited higher dielectric constants than the samples sintered in air. The reducing atmosphere of $p_{\text{O}_2} = 5 \times 10^2$ Pa had no effect on the piezoelectric properties of the BCTZ ceramics. Enhanced piezoelectric properties with peaked values of 200 pC/N for d_{33} and 17% for k_p were obtained for the BCTZ ceramics sintered in N₂ gas at 1350 °C. The piezoelectric properties of the BCTZ ceramics may be further optimized as a function of both phase structure and microstructure for their piezoelectric applications.

Acknowledgments

This work was supported by the High-Tech 863 Program of China (Grant No. 2006AA03Z436). Valuable advice from Professor Jing-Feng Li in Tsinghua University and the reviewers is gratefully acknowledged.

References

- Feng, Q. Q., McConville, C. J., Edwards, D. D., McCauley, D. E. and Chu, M., Effect of oxygen partial pressure on the dielectric properties and microstructures of co-fired base-metal-electrode multilayer ceramic capacitors. *J. Am. Ceram. Soc.*, 2006, **89**(3), 894–901.
- Uchino, K., Materials issues in design and performance of piezoelectric actuators: an overview. *Acta Mater.*, 1998, **46**(11), 3745–3753.
- Hennings, D. F. K. and Schreinemacher, H., Ca-acceptors in dielectric ceramics sintered in reductive atmospheres. *J. Eur. Ceram. Soc.*, 1995, **15**, 795–800.
- Kishi, H., Mizuno, Y. and Chazono, H., Base-metal electrode-multilayer ceramic capacitors: past, present and future perspectives. *Jpn. J. Appl. Phys.*, 2003, **42**, 1–15.
- Jain, T. A., Fung, K. Z. and Chan, J., Effect of the A/B ratio on the microstructures and electrical properties of (Ba_{0.95±x}Ca_{0.05})(Ti_{0.82}Zr_{0.18})O₃ for multilayer ceramic capacitors with nickel electrodes. *J. Alloy Compd.*, 2009, **468**, 370–374.
- Kington, A. I. and Srinivasan, S., Lead zirconate titanate thin films directly on copper electrodes for ferroelectric, dielectric and piezoelectric applications. *Nat. Mater.*, 2005, **4**, 233–237.
- Wu, A., Vilarinho, P. M., Srinivasan, S., Kington, A. I., Reaney, I. M., Woodward, D. et al., Microstructural studies of PZT thick films on Cu foils. *Acta Mater.*, 2006, **54**, 3211–3220.
- Saito, Y., Takao, H., Tani, T., Nonoyama, T., Takatori, K., Homma, T. et al., Lead-free piezoceramics. *Nature*, 2004, **432**, 84–87.
- Jiang, M. H., Liu, X. Y. and Chen, G. H., Phase structures and electrical properties of new lead-free Na_{0.5}K_{0.5}NbO₃–LiSbO₃–BiFeO₃ ceramics. *Scripta Mater.*, 2009, **60**(10), 909–912.
- Zuo, R. Z., Fu, J. and Lv, D., Phase transformation and tunable piezoelectric properties of lead-free (Na_{0.52}K_{0.48-x}Li_x)(Nb_{1-x-y}Sb_yTa_x)O₃ system. *J. Am. Ceram. Soc.*, 2009, **92**(1), 283–285.
- Zhang, Y. R., Li, J. F., Zhang, B. P. and Peng, C. E., Piezoelectric and ferroelectric properties of Bi-compensated (Bi_{1/2}Na_{1/2})TiO₃–(Bi_{1/2}K_{1/2})TiO₃ lead-free piezoelectric ceramics. *J. Appl. Phys.*, 2008, **103**, 074109.
- Takahashi, H., Numamoto, Y., Tani, J. and Tsurekawa, S., Piezoelectric properties of BaTiO₃ ceramics with high performance fabricated by microwave sintering. *Jpn. J. Appl. Phys.*, 2006, **45**(9), 7405–7408.
- Takahashi, H., Numamoto, Y., Tani, J., Matsuta, K., Qiu, J. H. and Tsurekawa, S., Lead-free barium titanate ceramics with large piezoelectric constant fabricated by microwave sintering. *Jpn. J. Appl. Phys.*, 2006, **45**(1), L30–L32.
- Shao, S. F., Zhang, J. L., Zhang, Z., Zheng, P., Zhao, M. L., Li, J. C. et al., High piezoelectric properties and domain configuration in BaTiO₃ ceramics obtained through the solid-state reaction route. *J. Phys. D: Appl. Phys.*, 2008, **41**, 125408.
- McCauley, D. E., Chu, M. and Megherhi, M. H., PO₂ dependence of the diffuse-phase transition in base metal capacitor dielectrics. *J. Am. Ceram. Soc.*, 2006, **89**(1), 193–201.
- Zhang, X. W., Han, Y. H., Lal, M. and Smyth, D. M., Defect chemistry of BaTiO₃ with additions of CaTiO₃. *J. Am. Ceram. Soc.*, 1987, **70**(2), 100–103.
- Hansen, P., Hennings, D. and Schreinemacher, H., Dielectric properties of acceptor-doped (Ba,Ca)(Ti,Zr)O₃ ceramics. *J. Electroceram.*, 1998, **2**(2), 85–94.
- Albertsen, K., Hennings, D. and Steigelmann, O., Donor–acceptor charge complex formation in barium titanate ceramics: role of firing atmosphere. *J. Electroceram.*, 1998, **2**(3), 193–198.

19. Cheng, X. and Shen, M., Different microstructure and dielectric properties of $\text{Ba}_{1-x}\text{Ca}_x\text{TiO}_3$ ceramics and pulsed-laser-ablated films. *Mater. Res. Bull.*, 2007, **42**(9), 1662–1668.
20. Nanakorn, N., Jalupoom, P., Vaneesorn, N. and Thanaboonsombut, A., Dielectric and ferroelectric properties of $\text{Ba}(\text{Zr}_x\text{Ti}_{1-x})\text{O}_3$ ceramics. *Ceram. Int.*, 2008, **34**, 779–782.
21. Cheng, B. L., Wang, C., Wang, S. Y., Lu, H. B., Zhou, Y. L., Chen, Z. H. et al., Dielectric properties of $(\text{Ba}_{0.8}\text{Sr}_{0.2})(\text{Zr}_x\text{Ti}_{1-x})\text{O}_3$ thin films grown by pulsed-laser deposition. *J. Eur. Ceram. Soc.*, 2005, **25**, 2295–2298.
22. Wu, Y. C., Wang, S. F., McCauley, D. E., Chu, M., Lu, S. H. and Yang, H., Dielectric behavior and second phases in X7R-formulated BaTiO_3 sintered in low-oxygen partial pressures. *J. Am. Ceram. Soc.*, 2007, **90**(9), 2926–2934.
23. Hennings, D. and Schreinemacher, H., Temperature dependence of the segregation of calcium titanate from solid solutions of $(\text{Ba,Ca})(\text{Ti,Zr})\text{O}_3$ and its effect on the dielectric properties. *Mater. Res. Bull.*, 1977, **12**(12), 1221–1226.
24. Chang, Y. F., Yang, Z. P., Hou, Y. T., Liu, Z. H. and Wang, Z. L., Effects of Li content on the phase structure and electrical properties of lead-free $(\text{K}_{0.46-x/2}\text{Na}_{0.54-x/2}\text{Li}_x)(\text{Nb}_{0.76}\text{Ta}_{0.20}\text{Sb}_{0.04})\text{O}_3$ ceramics. *Appl. Phys. Lett.*, 2007, **90**, 232905.
25. Dai, Y. J. and Zhang, X. W., Phase transition behavior and electrical properties of lead-free $(1-x)(0.98\text{K}_{0.5}\text{Na}_{0.5}\text{NbO}_3-0.02\text{LiTaO}_3)-x(0.96\text{Bi}_{0.5}\text{Na}_{0.5}\text{TiO}_3-0.04\text{BaTiO}_3)$ piezoelectric ceramics. *J. Eur. Ceram. Soc.*, 2008, **28**, 3193–3198.
26. Wu, J. G., Xiao, D. Q. and Wang, Y. Y., Effects of K/Na ratio on the phase structure and electrical properties of $(\text{K}_x\text{Na}_{0.96-x}\text{Li}_{0.04})(\text{Nb}_{0.91}\text{Ta}_{0.05}\text{Sb}_{0.04})\text{O}_3$ lead-free ceramics. *Appl. Phys. Lett.*, 2007, **91**, 242909.
27. Du, H. L., Zhou, W. C., Luo, F. and Zhu, D. M., An approach to further improve piezoelectric properties of $(\text{K}_{0.5}\text{Na}_{0.5})\text{NbO}_3$ -based lead-free ceramics. *Appl. Phys. Lett.*, 2007, **91**, 202907.
28. Ramam, K. and Lopez, M., Barium modified lead lanthanum strontium zirconium niobium titanate for dielectric and piezoelectric properties. *J. Eur. Ceram. Soc.*, 2007, **27**, 3141–3147.
29. Tkach, A., Vilarinho, P. M. and Kholkin, A. L., Dependence of dielectric properties of manganese-doped strontium titanate ceramics on sintering atmosphere. *Acta Mater.*, 2006, **54**, 5385–5391.
30. Zhuang, Z. Q., Harmer, M. P., Smyth, D. M. and Newnham, R. E., The effect of octahedrally-coordinated calcium on the ferroelectric transition of BaTiO_3 . *Mater. Res. Bull.*, 1987, **22**(10), 1329–1335.
31. Victor, P., Ranjith, R. and Krupanidhi, S. B., Normal ferroelectric to relaxor behavior in laser ablated Ca-doped barium titanate thin films. *J. Appl. Phys.*, 2003, **94**(12), 7702–7709.
32. Du, H. L. and Yao, X., Effects of Sr substitution on dielectric characteristics in $\text{Bi}_{1.5}\text{ZnNb}_{1.5}\text{O}_7$ ceramics. *Mater. Sci. Eng. B*, 2003, **99**, 437–440.
33. Abdeen, A. M., Dielectric behavior in Ni–Zn ferrites. *J. Magn. Magn. Mater.*, 1999, **192**, 121–129.
34. Chang, Y. F., Yang, Z. P. and Wei, L. L., Microstructure, density, and dielectric properties of lead-free $(\text{K}_{0.44}\text{Na}_{0.52}\text{Li}_{0.04})(\text{Nb}_{0.96-x}\text{Ta}_x\text{Sb}_{0.04})\text{O}_3$ piezoelectric ceramics. *J. Am. Ceram. Soc.*, 2007, **90**(5), 1656–1658.
35. Zhang, H. L., Li, J. F. and Zhang, B. P., Microstructure and electrical properties of porous PZT ceramics derived from different pore-forming agents. *Acta Mater.*, 2007, **55**, 171–181.
36. Ramam, K. and Lopez, M., Microstructure, dielectric and electromechanical properties of PLSZFT nanoceramics for piezoelectric applications. *J. Mater. Sci. Mater. Electron.*, 2008, **19**, 1140–1145.
37. Karaki, T., Yan, K., Miyamoto, T. and Adachi, M., Lead-free piezoelectric ceramics with large dielectric and piezoelectric constants manufactured from BaTiO_3 nano-powder. *Jpn. J. Appl. Phys.*, 2007, **46**(4), L97–L98.
38. Yang, G. Y., Lee, S. I., Liu, Z. J., Anthony, C. J., Dickey, E. C., Liu, Z. K. et al., Effect of local oxygen activity on Ni– BaTiO_3 interfacial reactions. *Acta Mater.*, 2006, **54**, 3513–3523.